

A COMPREHENSIVE ORBIT RECONSTRUCTION FOR THE GALILEO PRIME MISSION IN THE J2000 SYSTEM

R. A. Jacobson[†], R. J. Haw[‡], T. P. McElrath[‡], P. G. Antreasian[§]

Jet Propulsion Laboratory
California Institute of Technology
Pasadena, California 91109

The Galileo spacecraft began its orbital tour of the Jovian system in December of 1995 and completed its 11 orbit prime mission in November of 1997 having had 17 close encounters with the Galilean satellites. Earlier papers discussed the determination of the spacecraft orbit in support of mission operations from arrival at Jupiter through the first 9 orbits. In this paper we report on the reconstruction of the spacecraft trajectory for the entire prime mission, the development of a consistent set of ephemerides for the Galilean satellites, the improvement of the ephemeris of Jupiter, the determination of the gravity field of the Jovian system, and the determination of the orientation of the pole of Jupiter.

INTRODUCTION

The Galileo spacecraft arrived at Jupiter in December of 1995 to begin an orbital tour of the Jovian system. The objective of the tour was the study of the planet, its satellites, and its magnetosphere. The spacecraft completed its 11 orbit prime mission in November of 1997 having had 17 close encounters with the Galilean satellites (including two prior to Jupiter orbit insertion and one during the period of solar conjunction). Galileo continues to operate and will have made an additional 11 orbits of Jupiter by the date of this Conference. Orbits 12 through 25 constitute the Galileo Europa Mission (GEM) which ends in November of 1999. Earlier papers by Antreasian *et al.*¹ and Haw *et al.*² discussed the determination of the spacecraft orbit in support of mission operations from arrival at Jupiter through the first 9 orbits. The objective of the work described in this paper is the reconstruction of the spacecraft trajectory for the prime mission together with the development of a consistent set of ephemerides for the Galilean satellites. By necessity the work also includes the improvement of the Jupiter ephemeris, the values of the Jovian system gravitational parameters, and the Jupiter pole orientation angles. To enhance our ephemeris and gravity field improvements we incorporated data from a number of GEM orbits. However, we did not perform a complete spacecraft trajectory reconstruction for those orbits, but instead focused only on that portion of

[†]Member of the Technical Staff, Jet Propulsion Laboratory, Associate Fellow AIAA.

[‡]Member of the Engineering Staff, Jet Propulsion Laboratory

[§]Member of the Engineering Staff, Jet Propulsion Laboratory, Member AIAA

each orbit involving the satellite close encounter. Table 1 summarizes the geometry of the satellite encounters on each of the Galileo orbits included in the analysis.

Table 1: SATELLITE ENCOUNTER GEOMETRY AND TIMES

Satellite	Orbit	Alt.(km)	Lat.(deg)	Long.(deg)	Time (TDB)	
Europa	0	33001.1	-64.196	75.871	07-Dec-1995	13:09:53.10
Io	0	896.9	-9.562	259.060	07-Dec-1995	17:46:59.52
Ganymede	1	835.0	30.399	246.622	27-Jun-1996	06:30:08.86
Ganymede	2	261.1	79.293	236.324	06-Sep-1996	19:00:36.04
Callisto	3	1136.0	13.196	282.252	04-Nov-1996	13:35:29.87
Europa	3	34787.6	0.667	125.962	06-Nov-1996	18:50:53.37
Europa	4	692.1	-1.673	322.463	19-Dec-1996	06:53:59.93
Europa ¹	5	26667.9	-0.830	351.308	20-Jan-1997	01:09:39.47
Europa	6	586.3	-17.017	34.612	20-Feb-1997	17:07:12.41
Europa	7	23486.4	2.142	226.254	04-Apr-1997	05:59:49.81
Ganymede	7	3101.9	55.793	270.371	05-Apr-1997	07:11:00.30
Callisto	8	33059.9	-41.999	287.725	06-May-1997	12:11:25.00
Ganymede	8	1603.2	28.268	84.848	07-May-1997	15:57:11.74
Callisto	9	418.2	1.964	100.977	25-Jun-1997	13:48:52.15
Ganymede	9	79739.9	-0.017	261.228	26-Jun-1997	17:20:36.52
Callisto	10	535.3	4.607	281.292	17-Sep-1997	00:19:57.98
Europa	11	2043.3	25.732	218.710	06-Nov-1997	20:32:47.39
Ganymede	12	14402.6	-5.811	266.141	15-Dec-1997	09:59:12.54
Europa	12	201.0	-8.676	134.324	16-Dec-1997	12:04:23.06
Europa	14	1644.1	12.197	131.170	29-Mar-1998	13:22:08.33
Europa	16	1834.2	-25.653	133.602	21-Jul-1998	05:04:47.96
Europa	19	1439.4	30.515	28.157	01-Feb-1999	02:20:54.14
Callisto	20	1321.4	2.788	258.236	05-May-1999	13:57:22.29
Callisto	21	1048.1	-0.706	286.001	30-Jun-1999	07:47:53.87
Io	21	124362.8	0.448	222.231	02-Jul-1999	05:13:11.25

¹during solar conjunction

We also included data from the 1992 Ulysses Jupiter flyby^{3,4} to aid in our correction of the Jupiter ephemeris; we redetermined the Ulysses orbit in light of the corrected ephemerides, gravity field, and pole.

Unlike Galileo Mission Operations which works in the EME-1950 coordinate system, we elected to work in the (J2000) International Celestial Reference Frame (ICRF), the reference frame of the current JPL planetary and satellite ephemerides as well as the standard frame of the international astronomical and planetary science community. Use of this frame permits more precise modelling of the spacecraft and satellite observations. Moreover, it is the frame of choice for all other operational JPL missions and will probably be the frame for future missions for some time. Consequently, our adoption of the ICRF will facilitate the combination of our results with any obtained from future missions (e.g. the Europa Orbiter mission). In addition, our results may be used by the science community without need of a reference frame conversion.

The paper provides a discussion of the observation processing and its outcome. We examine the quality of the fit to the observations, and we give the values of the parameters in our dynamical model and their uncertainties. Also we compare our reconstructed orbits to the orbits determined during mission operations and our gravitational parameters to those appearing in the scientific literature.

ANALYSIS

Model

To determine the orbits of the spacecraft, planet, and satellites we adjusted parameters in the dynamical model of their motions to obtain a least squares fit to observations. The motion model includes gravitational dynamics (attractions of the satellites, Jupiter, the Sun, and other solar system planets) which affect the spacecraft, planet, and satellites and non-gravitational dynamics (solar radiation pressure and thrusting maneuvers) which affect only the spacecraft.

JPL planetary ephemeris DE405⁵ provided the positions and masses of the bodies in the solar system. The initial masses of the bodies in the Jovian system were from Campbell and Synnott⁶ (Note: the DE405 Jovian system mass is the Campbell and Synnott mass).

The gravity fields of the planet and satellites were represented by the standard spherical harmonic expansion of their gravitational potentials. For Jupiter we used only the first three even zonal harmonic coefficients with their initial values taken from Campbell and Synnott⁶. The extent of the satellite gravity fields was dictated by the number of close approaches and their altitudes. We adopted a complete second degree and order field for Io, third degree and order fields for Europa and Callisto, and a fourth degree and order field for Ganymede. The initial values for all of the satellite gravity harmonic coefficients were set to zero except for J_2 and C_{22} which were taken from Zharkov *et al.*⁷ for uniform density satellites in hydrostatic equilibrium (Note: this implies $3J_2 = 10C_{22}$). We took the body axes orientation angles for Jupiter and its satellites from Davies *et al.*⁸.

The fundamental adjustable parameters included:

- epoch position and velocity of the spacecraft and each Galilean satellite
- orbital elements of Jupiter (i.e., the corrections to DE405)
- GM's of the planetary system and the Galilean satellites
- gravitational harmonics of the planet and Galilean satellites
- Jupiter pole orientation angles
- specular and diffuse reflectivities in the Galileo spacecraft solar radiation pressure model
- scaling factor for the Ulysses spacecraft solar radiation pressure model
- thrust magnitude and direction for large spacecraft maneuvers
- impulsive velocity changes for small spacecraft maneuvers

Data

The orbital motion models were fit to the following observation types:

- Galileo and Ulysses Doppler tracking
- Ulysses radiometric ranging
- Galileo and Ulysses very-long baseline interferometry (VLBI)
- Galileo optical navigation imaging
- Galileo occultations by the satellites
- satellite photometric Earthbased astrometry
- satellite CCD Earthbased astrometry
- satellite mutual events (mutual eclipses and occultations)
- satellite eclipse timings (eclipses by Jupiter)
- satellite positions from Voyager spacecraft imaging

With the exception of the Galileo VLBI data, the basic Galileo and Ulysses data and their calibrations have been discussed previously^{1,3}. Spacecraft VLBI observations, which measure the angular separations between the spacecraft and nearby quasars, are essentially no different for Galileo and Ulysses. We used the IERS quasar locations⁹ in our analysis. The Galileo optical navigation data (satellite images against a star background) was originally referenced to a star catalogue in the EME-1950 system. We modified them, replacing the reference star locations with J2000 positions from

the Hipparcos and Tycho catalogs (fortunately the stars appeared in at least one of these catalogs). The new positions are the best available J2000 positions of the stars. The occultation data are the times at which the spacecraft disappears (ingress) and reappears (egress) from behind a satellite as seen from the Earth. The times, determined by monitoring the loss and re-acquisition of radio transmissions from the spacecraft, were provided by the Galileo Radio Science Team¹⁰.

The photographic satellite observations are relative positions of the satellites measured by D. Pascu of the U.S. Naval Observatory over the period 1967-1993¹¹. The CCD observations are astrometric positions of the satellites obtained by the U.S. Naval Observatory Flagstaff Station¹²⁻¹⁶ for the period (1993-1998); the early data was provided in the form of the actual CCD measures, but the 1998 data was reduced to right ascension and declination positions. The mutual event observations are relative positions derived from the eclipses and occultations of the satellites by one another¹⁷⁻²³. The eclipse timings are the times at which the satellites enter and exit Jupiter eclipse. Although the history of these timings extends back to 1652, we used only those from 1967 to 1996²⁴⁻²⁶. The eclipse timings prior to 1990 were obtained either visually or photographically; the later eclipse times were deduced from CCD measurements. The Voyager data are satellite positions as seen from the Voyager spacecraft in 1979 derived from optical navigation imaging²⁷. Lieske²⁸ discusses most of the satellite observations in connection with the revision of his analytical theory of the Galilean satellites' motion. We included a number of observations acquired subsequent to Lieske's work.

In order to obtain an adequate fit to the observations we had to adjust a number of parameters in the observation model. These included:

- one-way Doppler bias and drift
- two-way Doppler biases (Ulysses only)
- station dependent range biases (Ulysses only)
- Galileo camera pointing

As in the case of the data, the nature of these parameters has been discussed previously^{1,3}.

Method of Solution

We processed the Galileo spacecraft data for each orbit separately, i.e., we determined an epoch state vector for each. In order to force a degree of continuity between the contiguous prime mission orbits, we imposed an equality constraint, in a least squares sense, on the spacecraft positions at the beginning and end times of each orbit. Orbit 0 (the Io encounter) is disjoint from the other orbits as we made no attempt to account for the Jupiter orbit insertion maneuver. The Io encounter is included because it provides significant information on Io's orbit and gravity field.

For the data from each Galileo orbit and the Ulysses encounter, we used the JPL Orbit Determination Program (ODP) to produce weighted observation partial derivatives and the weighted residual vectors and to pack them into an upper triangular square root information matrix and associated residual vector. This matrix and vector constitute the square root information array which is equivalent to the normal equations used in classical least squares data processing. Each column of the matrix and each element of the vector are associated with an adjustable parameter. We used the JPL Satellite Data Processing Software (SATDPS) to produce an analogous square root information array for the Galilean satellite observations.

The Galileo and Ulysses Doppler weights were set separately for each DSN pass to correspond to an accuracy of 2.5 times the root-mean-square (rms) of the residuals for that pass. However, no Doppler was weighted tighter than 0.2 mm/sec. The weights for the Ulysses range represented an accuracy of 5 meters, for the Galileo imaging an accuracy of 0.35 pixels, and for the Galileo occultations accuracies of from 1 to 3 seconds as recommended by the Radio Science Team. Initially the weights on the Ulysses and Galileo VLBI data corresponded to measurement accuracies of 1.5 ns. However, after considerable experimentation we found that we needed to weight the Galileo VLBI

a factor of 10 tighter to obtain a reasonable fit. With multiple data types, data weights effectively balance the information provided by each type. We speculate that the tighter weights on the Galileo VLBI were necessary because there were relatively few VLBI measurements and their contribution was being overwhelmed by the large number of Doppler measurements. The Earthbased satellite data were divided into sets according to data type and the observing period in which they were acquired. The weights for each set represented an accuracy of about 3 times the rms of the residuals for the set. Similarly, the Voyager 1 and 2 data weights were based on accuracy of 3 times the rms of their respective residuals.

The parameters in each square root information array can be grouped into two distinct sets: those unique to the array (e.g. maneuvers), and those common to two or more arrays (e.g. satellite GM's). Taking advantage of this grouping, we simplified our solution process by breaking it into two steps according to the technique described by Curkendall²⁹. The first step removes the unique parameters from each array, combines the separate arrays (via Householder transformations, see Lawson and Hanson³⁰) to obtain a composite array for the common parameters, and solves for the corrections to those common parameters. The second step solves for the unique parameters in each array given the solution for the common parameters. All solutions were generated by means of singular value decomposition techniques³⁰ applied to the square root information arrays. The primary advantage of this two step solution process is that the dimensionality of the estimation does not become unwieldy as the number of included Galileo orbits grows. The size of the common parameter set is effectively independent of the number of Galileo orbits, and each Galileo orbit may be analyzed separately once the common parameters have been determined.

In the solution process we also included a priori information on the spacecraft non-gravitational dynamical parameters, the observational model parameters, the Jupiter orbital elements, and the gravity field parameters. The selection of the a priori values and uncertainties on the spacecraft dynamical and observational parameters followed that used by McElrath *et al.*³ for Ulysses and Antreasian *et al.*¹ for Galileo. Standish³¹ provided a priori information on the Jupiter orbit based on the observations used to develop the DE405 planetary ephemeris. For the planet and satellite masses and the planetary zonal harmonics we obtained the a priori values and uncertainties from Campbell and Synnott⁶. We set the a priori values for the satellites' J_2 and C_{22} to the hydrostatic equilibrium values with uncertainties of 100%. Also to account for the hydrostatic equilibrium condition, we imposed an a priori correlation of 1.0 between the J_2 and C_{22} uncertainties. For all of the other satellite gravity harmonic coefficients the a priori values were set to zero. The coefficients C_{21} , S_{21} , and S_{22} all vanish if the satellite's body axes are aligned with its principal axes of inertia. We set their a priori uncertainties to reflect a 5 degree misalignment. At the suggestion of the Galileo Radio Science Team we set the normalized³² a priori uncertainties in all of the higher degree and order harmonics to $(0.0 \pm 5.0) \times 10^{-6}$.

RESULTS

Fit Quality

The statistics of the data fit residuals which appear in Table 2 confirm that all of the data is fit quite well. In general the Doppler, both Galileo and Ulysses, fits to a fraction of a meter per second; largest Doppler residuals are from Galileo orbits near periods of solar conjunction (Io, E4/E6, C20) where solar plasma effects are most pronounced. Figures 1-4 display the Galileo Doppler residuals for a selected sample of the orbits. The top part of each figure shows the residuals for the entire orbit; the bottom part concentrates on the one hour period centered near the satellite encounter time (the vertical arrow indicates the time of closest approach). The figures give an indication of typical tracking coverage and noise level variations. The high noise data is for the most part 1-way Doppler which is more than twice as noisy as 2-way/3-way; the high noise on the approach to Io is due to solar plasma. The noise also increases during the satellite flybys where Doppler compression

times are shorter; compression times are typically 60 seconds, but are reduced to 10 seconds for the two hour period around each satellite encounter. The close encounter residuals appearing in the bottom half of each figure give an indication of how well the satellite gravity fields are determined. No obvious signatures remain which can be attributed to gravitational mismodelling (analysis has found that the apparent oscillations in the Europa 12 residuals cannot be removed with reasonable changes to the gravity field).

Table 2: RESIDUAL STATISTICS

Type (units)	No. ¹	Mean	Sigma	Mean	Sigma	RMS
Io Doppler (mm/sec)	7992	0.043	2.118			2.118
G1A Doppler (mm/sec)	5638	-0.006	0.322			0.322
G1B Doppler (mm/sec)	12578	-0.032	0.672			0.672
G2 Doppler (mm/sec)	21324	0.003	0.252			0.252
C3 Doppler (mm/sec)	20611	0.002	0.301			0.301
E4 Doppler (mm/sec)	15774	-0.018	0.992			0.992
E6 Doppler (mm/sec)	20556	0.040	1.776			1.777
G7 Doppler (mm/sec)	18927	-0.014	0.307			0.308
G8 Doppler (mm/sec)	22327	-0.008	0.294			0.294
C9 Doppler (mm/sec)	19317	0.001	0.259			0.259
C10 Doppler (mm/sec)	34277	-0.001	0.291			0.291
E11 Doppler (mm/sec)	18031	-0.007	0.315			0.315
E12 Doppler (mm/sec)	14699	-0.010	0.342			0.342
E14 Doppler (mm/sec)	9586	0.014	0.668			0.668
E16 Doppler (mm/sec)	14110	0.000	0.130			0.130
E19 Doppler (mm/sec)	17505	0.008	0.620			0.620
C20 Doppler (mm/sec)	14131	-0.007	1.024			1.024
C21 Doppler (mm/sec)	11742	-0.006	0.235			0.235
Ulysses Doppler (mm/sec)	9269	-0.005	0.087			0.087
Ulysses Range (m)	4995	-0.004	0.675			0.675
Ulysses VLBI (ns)	31	-0.12	1.08			1.09
Galileo VLBI (ns)	24	-0.24	1.35			1.35
Galileo Occult. (sec)	18	0.19	1.38			1.36
Galileo Imaging ² (pixel)	105	0.025	0.154	-0.061	0.146	0.157
Sat. Photo ³ (arcsec)	4221	-0.000	0.089	-0.001	0.090	0.090
Sat. CCD ² (pixel)	872	0.000	0.044	0.000	0.058	0.052
Sat. CCD ³ (arcsec)	151	0.003	0.061	0.004	0.070	0.066
Sat. Mutual Events ³ (arcsec)	554	0.006	0.028	0.007	0.033	0.031
Sat. Eclipses - visual/photo (sec)	2117	-2.30	50.9			50.9
Sat. Eclipses - CCD (sec)	102	-4.04	17.3			17.7
Sat. Voyager 1 ⁴ (km)	108	-29.9	39.3	-17.5	40.3	46.6
Sat. Voyager 2 ⁴ (km)	73	-20.0	40.7	-2.3	30.2	38.4

¹number of measurements or measurement pairs

²separate statistics for line and pixel measures

³separate statistics for relative right ascension and declination measures

⁴separate statistics for absolute right ascension and declination measures

The statistics suggest that the Ulysses range is known to a fraction of a meter. The residuals, however, include adjustments from the range biases which are of the order of 5 to 10 meters.

The VLBI residuals are consistent with their presumed accuracy. They correspond position accuracies of 26 km and 33 km for Ulysses and Galileo, respectively, relative to the quasars at the times of the measurements (a 1 nanosecond accuracy is roughly 24 km).

The satellite photographic observations are fit to slightly better than the typical accuracy of such observations, 0.1 to 0.2 arcsec which is 300 to 600 km at Jupiter, and the satellite CCD observations are fit surprisingly well. The pixel and line form of these observations fits at about the 0.05 pixel or 50 km level (1 pixel roughly subtends 0.325 seconds of arc) while the astrometric form fits to about 0.07 arcsec or 200 km. The mutual events and eclipses also exhibit somewhat smaller residuals than expected. The Voyager residuals are totally consistent with their presumed accuracy.

Table 3 shows the position discontinuities at the junctions between the Galileo orbits; they are all less than 500 m (note: for computational convenience the E4/E6 constraint during solar conjunction was not imposed).

Table 3: GALILEO ORBIT DISCONTINUITIES (meters)

Junction	X	Y	Z
01-Jun-1996 (G0/G1)	-12	-8	-4
04-Aug-1996 (G1/G2)	105	-460	-205
12-Sep-1996 (G2/C3)	20	-76	-58
24-Nov-1996 (C3/E4)	107	-107	-45
16-Jan-1997 (E4/E6)	solar conjunction		
13-Mar-1997 (E6/G7)	79	-60	-31
21-Apr-1997 (G7/G8)	149	-30	-16
04-Jun-1997 (G8/C9)	-89	-15	-10
12-Jul-1997 (C9/C10)	-261	186	85
22-Sep-1997 (C10/E11)	-6	16	16
10-Nov-1997 (E11/E12)	28	-82	-26

Dynamical Parameters

The planetary system and Galilean satellite masses are given in Table 4. The differences between the Galileo values and those found with the Voyager data by Campbell and Synnott are within the latter's uncertainties. The Galileo uncertainties, however, are considerably reduced from those of Voyager.

Table 4: GM SOLUTIONS (km^3/sec^2)

Body	Voyager	Galileo
System	126712767. \pm 100.	126712762.53 \pm 2.00
Io	5961. \pm 10.	5959.70 \pm 0.10
Europa	3201. \pm 10.	3202.70 \pm 0.02
Ganymede	9887. \pm 3.	9887.85 \pm 0.04
Callisto	7181. \pm 3.	7179.28 \pm 0.03

Table 5 summarizes the gravitational harmonics found in this analysis together with the a priori values and those previously published. Only the second order and degree harmonics are shown for the satellites; the higher orders and degrees are small, of the the order of the a priori uncertainties, and

will not be discussed in this paper. Clearly the satellite gravity fields are considerably different from the a priori assumption of uniform density objects in hydrostatic equilibrium. In addition the S_{22} values suggest a body axes misalignment of a few degrees for Io and Europa. Our current values also differ significantly from those published by the Galileo radio scientists^{33–38}. The primary reasons for the difference are the inclusion of data from additional Galileo orbits (the radio science results are based on only the first 12 orbits) and a change in data processing procedure. Earlier work estimated biases and ionosphere calibration corrections for the Galileo Doppler data. Subsequent examination of the data found no strong evidence for the existence of the biases or the need for corrections to the ionosphere calibrations. Moreover, omitting them had little effect on the determination of the spacecraft orbit. Their presence, on the other hand, did affect the gravitational harmonic determination, i.e., the estimation process tended to fit the Doppler data by changing the biases and corrections rather than the harmonics. Therefore, we decided to eliminate the biases and ionosphere corrections from our analysis. Only the second zonal harmonic was estimated for Jupiter; it was found to be close to the value determined from the Voyager data but its uncertainty was considerably smaller. We made attempts to determine the higher order harmonics but could obtain no improvement over the Voyager results.

Table 5: GRAVITATIONAL HARMONICS (units of $\times 10^{-6}$)

Satellite	J_2	C_{21}	S_{21}	C_{22}	S_{22}	Source
Io	2150.±2150.	0.0±15.	0.±75.	664.±664.	0.±112.	a priori
	1863.± 90.			559.± 27.		Ref. 32
	1907.± 140.	0.1±15.	38.±74.	571.± 42.	-121.± 30.	Galileo
Europa	629.± 629.	0.0±4.4	0.±22.	189.±189.	0.± 33.	a priori
	436.± 8.	-1.4±6.0	14.±12.	131.± 3.	-12.± 3.	Ref. 36
	417.± 6.	-1.3±3.8	11.±10.	125.± 2.	-10.± 2.	Galileo
Ganymede	240.0±240.0	0.0±1.7	0.0±8.5	72.1±72.1	0.0±12.8	a priori
	127.4± 2.7			38.2± 0.9		Ref. 33
	135.1± 3.8	-0.4±1.4	-10.0±4.4	40.6± 1.1	1.0± 2.3	Galileo
Callisto	44.6± 44.6	0.0±0.3	0.0±1.6	14.0±14.0	0.0± 2.5	a priori
	47.7± 11.5			14.3± 3.2		Ref. 34
	31.1± 4.5	0.0±0.4	0.0±0.8	10.5± 0.4	-0.7± 0.3	Ref. 35
	36.4± 1.8	0.0±0.3	0.1±1.6	11.4± 0.6	-2.0± 0.9	Galileo
Jupiter	14736.00± 1.00					Voyager
	14735.36± 0.03					Galileo

Reference radii (km): Io (1821.3), Europa (1565.0), Ganymede (2634.0), Callisto (2403.0)
Jupiter (71398.0)

The revised Jupiter pole orientation is given in Table 6 together with the pole adopted by the IAU⁸ and the pole from the E5 Galilean satellite theory²⁸ (transformed to J2000). We took our pole rates from that theory. The IAU pole orientation is from Null’s analysis of the Pioneer 10 and Pioneer 11 tracking data³⁹ with rates derived from the E2 Galilean satellite theory⁴⁰. Both the angles and rates were transformed from the B1950 system to the J2000 system by the IAU in 1983. The E5 pole is from Campbell and Synnott’s analysis of the Voyager data⁶. Our pole is in good agreement with the transformed E5 pole, is an order of magnitude more accurate, and offers a significant improvement over the IAU pole.

Orbit Comparisons

Figure 5 compares a concatenation of the reconstructed Galileo orbits with a concatenation of orbits produced by the Galileo Navigation Team. The three parts of the figure show the Jupiter

Table 6: JUPITER POLE PARAMETERS (at Julian Date 2451545.0)

Source	$\alpha(\text{deg})$	$\dot{\alpha}(\text{deg/cty})$	$\delta(\text{deg})$	$\dot{\delta}(\text{deg/cty})$
IAU1996	268.050 \pm 0.016	-9.0×10^{-3}	64.490 \pm 0.004	3.0×10^{-3}
E5(J2000)	268.056 \pm 0.005	-7.2439×10^{-3}	64.495 \pm 0.001	2.7147×10^{-3}
Galileo	268.0572 \pm 0.0006	-7.2439×10^{-3}	64.4951 \pm 0.0001	2.7147×10^{-3}

relative position differences along the spacecraft orbital track, along the spacecraft orbital radial direction, and normal to the spacecraft orbital plane. The large vertical ticks on the abscissa of part c denote the times of the close satellite encounters. Since the reconstruction is continuous to the 500 meter level, the jumps seen in the figure (e.g., on 21 August 1996) are a consequence of discontinuities between contiguous Navigation produced orbits. Sharp turns (e.g., on 14 March 1996) are associated with spacecraft maneuvers which have reconstructed values slightly different than the values found by the Navigation Team (this is particularly true for the out-of-plane maneuver components). The largest trajectory differences occur in the out-of-plane direction and represent orientation differences between the two orbital planes. This is not a surprising result as the orbit plane orientation is difficult to determine from spacecraft tracking data. The large out-of-plane difference in early 1996 is a consequence of data processing differences. The Navigation orbit actually began on 12 December 1995, included the sparse and very noisy Doppler in December, and contained two maneuvers in December. The reconstruction orbit began on the 1 January 1996. Apparently the December data coupled with the maneuvers produced significantly different spacecraft orbits. After the maneuvers in mid-March 1996, the two orbits began to move into closer agreement. It is interesting to note that both orbits fit the same Doppler data from January to June, consequently the differences are a clear example of the insensitivity of the Doppler data to the orbit plane orientation.

Figure 6 compares the corrected Jupiter ephemeris with DE405 in terms of position differences in the orbital in-track, radial, and out-of-plane directions. The secular trend in the downtrack difference corresponds to an orbital period difference of about 5 seconds. Our data arc, however, covers only about one half of a Jupiter orbit (Ulysses in 1992 to Galileo in 1998) and cannot provide a good estimate of the orbital period. On the other hand, the 5 second difference is of the order of the uncertainty in the DE405 Jupiter period which implies that we have not made an unreasonable change to the period. In the out-of-plane direction a significant periodic difference appears which reflects a difference in the orientation of the Jupiter orbital planes. The 80 km amplitude of the difference, however, is considerably less than the 200 to 300 km position uncertainty due to the uncertainty in the DE405 Jupiter orbital plane orientation.

Figures 7–10 provide comparisons between the Galilean satellite orbits and the pre-mission orbits provided to the Navigation Team⁴¹. The differences give an indication of the changes introduced by the addition of the Galileo data as well as the post-1995 Earthbased satellite observations. The differences are all periodic with some offset in the Ganymede and Callisto in-orbit positions. Consequently, we can conclude that the orbital periods were changed little by the Galileo data. The amplitudes of the differences are well within the 100 to 200 km uncertainty of the pre-Galileo orbits.

We believe that the Galilean satellite orbits are known to about 5 km ($1-\sigma$) through out the Galileo mission (December 1995 to July 1999). Outside the mission time frame the accuracy is expected to degrade somewhat with the error growth primarily in the in-orbit direction due to the orbital period error.

At the time of each satellite encounter the Galileo spacecraft position relative to the satellite is known to better than 1 km due to the strong gravitational tie sensed by the Doppler data. See Antreasian *et al.*¹ for a discussion of typical encounter accuracies. Since the spacecraft is so tightly tied to the satellite, the spacecraft position relative to Jupiter at those times may be presumed to have the same accuracy as the satellite position, 5 km ($1-\sigma$). Away from the satellite encounters,

however, knowledge of the spacecraft orbit degrades, especially in view of the many maneuvering events and the acknowledged difficulty in determining orbital plane orientation from Doppler data. We made a rough estimate of the orbit accuracy away from the encounters by examining the stability of the orbit solutions as more data was added and various processing strategies were employed. We also took into account the comparison with the operational orbits, Figure 5, recalling that those orbits were produced independently in a different reference system with a different processing technique. We conclude that in-orbit and radial errors are probably not much larger than 5 km and that the out-of-plane errors are the most significant. The out-of-plane error may be considered primarily an error in orbital inclination and will vary along the orbit depending on tracking data availability, data quality, maneuver schedule, maneuver size, and maneuver execution error. We expect the error to range between 5 and 50 km.

Our Ulysses results are basically a repeat of the work of McElrath *et al.*³. We estimate the accuracy of our Ulysses trajectory at the time of Jupiter encounter to be 2–3 km.

The Jupiter orbit corrections are an indirect consequence of processing the spacecraft Doppler, range, and VLBI data. The VLBI measures the spacecraft relative to the quasars, and the Doppler and range measure the spacecraft relative to the Earth (the location of the Earth relative to the quasars is quite well known⁵). It is the gravitational tie of the spacecraft to Jupiter which leads to the Jupiter orbit corrections. The accuracy of our Jupiter ephemeris, therefore, is limited by our knowledge of the spacecraft orbit. Through out the Galileo mission time frame we believe that our ephemeris is probably good to the level of the corrections: 10 km radially, 50 km along the orbit, and 75 km out-of-plane. At the time of the Ulysses encounter, however, the Jupiter position accuracy is about the same as previously determined^{3,4}, 1 km, 10 km, and 15 km in those respective directions.

CONCLUDING REMARKS

This paper has reported on a reconstruction of the spacecraft trajectory for the Galileo prime mission, the development of associated ephemerides for the Galilean satellites and Jupiter, the determination of the gravity field of the Jovian system, and the determination of the orientation of the pole of Jupiter. The Galileo mission (GEM) is expected to continue for some time, and we will use the data acquired from this continuation to further improve the ephemerides and gravity field. The results of those improvements will appear in future scientific publications. Because refinement of the ephemerides and gravity parameters affects the spacecraft orbit, we expect to make small changes in the prime mission reconstruction as the additional data is processed. There are no plans, however, to produce a continuous reconstruction for the entire GEM mission. The GEM data analysis will concentrate only on the portions of the spacecraft orbits in the vicinity of the satellite encounters (i.e., analysis will be done in the same manner as for orbits 14, 16, 19–21).

ACKNOWLEDGEMENT

We would like to thank Mike Wang and Claude Hildebrand for processing the original Galileo optical data and Bill Owen for his assistance in converting it to the J2000 system. The research described in this paper was performed at the Jet Propulsion Laboratory, California Institute of Technology, under contract with the National Aeronautics and Space Administration.

REFERENCES

1. Antreasian, P.G., McElrath, T.P., Haw, R.J., & Lewis, G.D. (1997) 'Galileo Orbit Determination Results During the Satellite Tour', AAS Paper No. 97-699, AAS/AIAA Astrodynamics Specialist Conference, Sun Valley, Idaho.

2. Haw, R.J., Antreasian, P.G., Graat, E.G., McElrath, T.P., & Nicholson, F.T. (1997) 'Navigating Galileo at Jupiter Arrival', *AIAA Journal of Spacecraft and Rockets* **34**, No. 4, pp. 503.
3. McElrath, T.P., Tucker, B., Criddle, K. E., Menon, P. R., & Higa, E. S. (1992) 'Ulysses Navigation at Jupiter Encounter', AIAA Paper No. 92-4524, AIAA/AAS Astrodynamics Conference, Hilton Head, South Carolina.
4. Folkner, W. M., McElrath, T.P., & Mannucci, J. (1996) 'Determination of Position of Jupiter from Very-Long Baseline Interferometry Observations of Ulysses', *The Astronomical Journal* **112**, pp. 1294-1297.
5. Standish, E. M. (1998) 'JPL Planetary and Lunar Ephemerides, DE405/LE405', JPL Internal Document IOM 312.F-98-048.
6. Campbell, J. K. & Synnott, S. P. (1985) 'Gravity Field of the Jovian System from Pioneer and Voyager Tracking Data', *The Astronomical Journal* **90**, pp. 364-372.
7. Zharkov, V. N., Leontjev, V. V., & Kozenko, A. V. (1985) 'Models, Figures, and Gravitational Moments of the Galilean Satellites of Jupiter and Icy Satellites of Saturn', *Icarus* **61**, pp. 92-100.
8. Davies, M. E., Abalakin, V. K., Bursa, M., Lieske, J. H., Morando, B., Morrison, D., Seidelmann, P., K., Sinclair, A. T., Yallop, B., & Tjuffin, Y. S. (1996) 'Report of the IAU/IAG/COSPAR Working Group on Cartographic Coordinates and Rotational Elements of the Planets and Satellites:1994', *Celestial Mechanics and Dynamical Astronomy* **63** pp. 127-148.
9. Ma, C., Arias, E.F., Eubanks, T.M., Fey, A.L., Gontier, A.-M., Jacobs, C.S., Sovers, O.J., Archinal, B.A., Charlot, P. (1997) 'The International Celestial Reference Frame realized by VLBI', IERS Technical Note 23, Part II, C. Ma and M. Feissel (eds.), Observatoire de Paris.
10. Klore, A. (1998) private communication of radio science satellite occultation times.
11. Pascu, D. (1993) private communication of satellite observations.
12. Monet, A. (1994) private communication of satellite observations.
13. Monet, A. (1995) private communication of satellite observations.
14. Monet, A. (1996) private communication of satellite observations.
15. Monet, A. (1997) private communication of satellite observations.
16. Stone, R. (1999) private communication of satellite observations.
17. Aksnes, K. & Franklin, F. A. (1976) 'Mutual Phenomena of the Galilean Satellites in 1973. III. Final results from 91 light curves', *The Astronomical Journal* **81** pp. 464-481.
18. Aksnes, K., Franklin, F. A., Millis, R., Birch, P., Blanco, C., Catalano, S., & Piironen, J. (1984) 'Mutual Phenomena of the Galilean and Saturnian Satellites in 1973 and 1979/1980', *The Astronomical Journal* **89** pp. 280-288.
19. Descamps, P. (1994) 'Astrometric analysis of Europa-Io occultations observed in 1991', *Astronomy and Astrophysics* **291** pp. 664-667.
20. Franklin, F. A. (1991) 'An Analysis of the 1985 Observations of Mutual Phenomena of the Galilean Satellites', *The Astronomical Journal* **102** pp. 806-814.
21. Goguen, J. D. (1994) private communication of satellite observations.
22. Kaas, A. A., Aksnes, K., Franklin, F. A. & Lieske, J. (1999) 'Astrometry from Mutual Phenomena of the Galilean Satellites in 1990-1992', *The Astronomical Journal* **117** pp. 1933-1941.
23. Spencer, J. (1993) private communication of satellite observations.
24. Lieske, J. H. (1986) 'A Collection of Galilean satellite eclipse observations, 1652-1983: Part I', *Astronomy and Astrophysics* **154** pp. 61-76.
25. Lieske, J. H. (1986) 'A Collection of Galilean satellite eclipse observations, 1652-1983: II', *Astronomy and Astrophysics Supplement Series* **63** pp. 143-202.
26. Mallama, A. (1997) private communication of Jupiter eclipses.
27. Synnott, S. P., Donegan, A. J., & Morabito, L. A. (1982) 'Position Observations of the Galilean Satellites from Voyager Data', JPL internal document.
28. Lieske, J. H. (1998) 'Galilean satellite ephemerides E5', *Astronomy and Astrophysics Supplement Series* **129** pp. 205-217.
29. Curkendall, D. W. (1973) 'On Combining Estimates with the Householder Machinery' JPL Internal Document IOM 391.2-399.
30. Lawson, C.L., Hanson, R.J. 1974, *Solving Least Squares Problems*, Prentice-Hall, Englewood Cliffs, N.J.

31. Standish, E. M. (1998) private communication of Jupiter ephemeris information.
32. Kaula, W. M. (1966) *Theory of Satellite Geodesy*, Blaisdell, Waltham, MA.
33. Anderson, J.D., Sjogren, W.L., & Schubert, G. (1996) 'Galileo Gravity Results and the Internal Structure of Io', *Science* **272** pp. 709-712.
34. Anderson, J.D., Lau, E.L., Sjogren, W.L., Schubert, G., & Moore, W.B. (1996) 'Gravitational constraints on the internal structure of Ganymede', *Nature* **384** pp. 541-543.
35. Anderson, J.D., Lau, E.L., Sjogren, W.L., Schubert, G., & Moore, W.B. (1997) 'Gravitational evidence for an undifferentiated Callisto', *Nature* **387** pp. 264-266.
36. Anderson, J.D., Schubert, G., Jacobson, R.A., Lau, E.L., Moore, W.B., & Sjogren, W.L. (1998) 'Distribution of Rock, Metals, and Ices in Callisto', *Science* **280** pp. 1573-1576.
37. Anderson, J.D., Schubert, G., Jacobson, R.A., Lau, E.L., Moore, W.B., & Sjogren, W.L. (1998) 'Europa's Differentiated Internal Structure: Inferences from Four Galileo Encounters', *Science* **281** pp. 2019-2022.
38. Anderson, J.D., Jacobson, R.A., Lau, E.L., Sjogren, W.L., Schubert, G., & Moore, W.B. (1998) 'Interior Structure of the Galilean Satellites', *1998 Bull. AAS* **30**, No. 2, 826
39. Null, G. W. (1976) 'Gravity field of Jupiter and its satellites from Pioneer 10 and Pioneer 11 tracking data', *The Astronomical Journal* **81** pp. 1153-1161.
40. Lieske, J. H. (1980) 'Improved Ephemerides of the Galilean Satellites', *Astronomy and Astrophysics* **82** pp. 340-348.
41. Jacobson, R. A. (1995) 'Integrated Ephemerides of the Galilean Satellites', JPL Internal Document IOM 314.10-125.

Fig. 1a Doppler Residuals – Io orbit 0

No.= 7992 rms= 2.11852

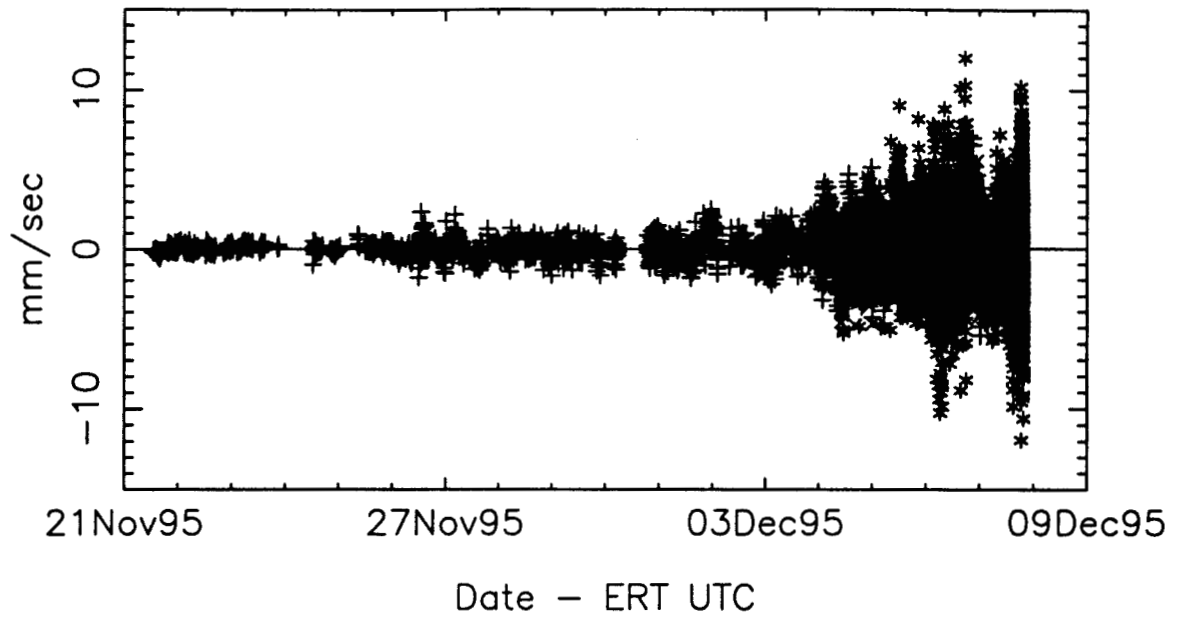


Fig. 1b Doppler Residuals – Io encounter

No.= 357 rms= 3.79513

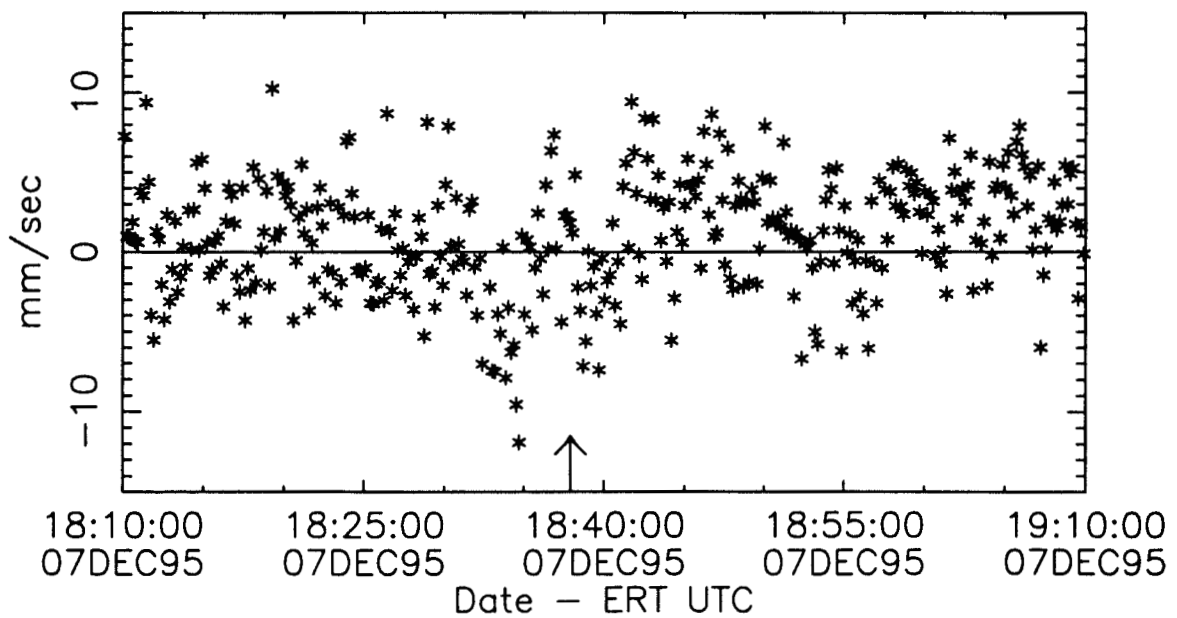


Fig. 2a Doppler Residuals – Ganymede orbit 2

No.= 21324 rms= 0.252414

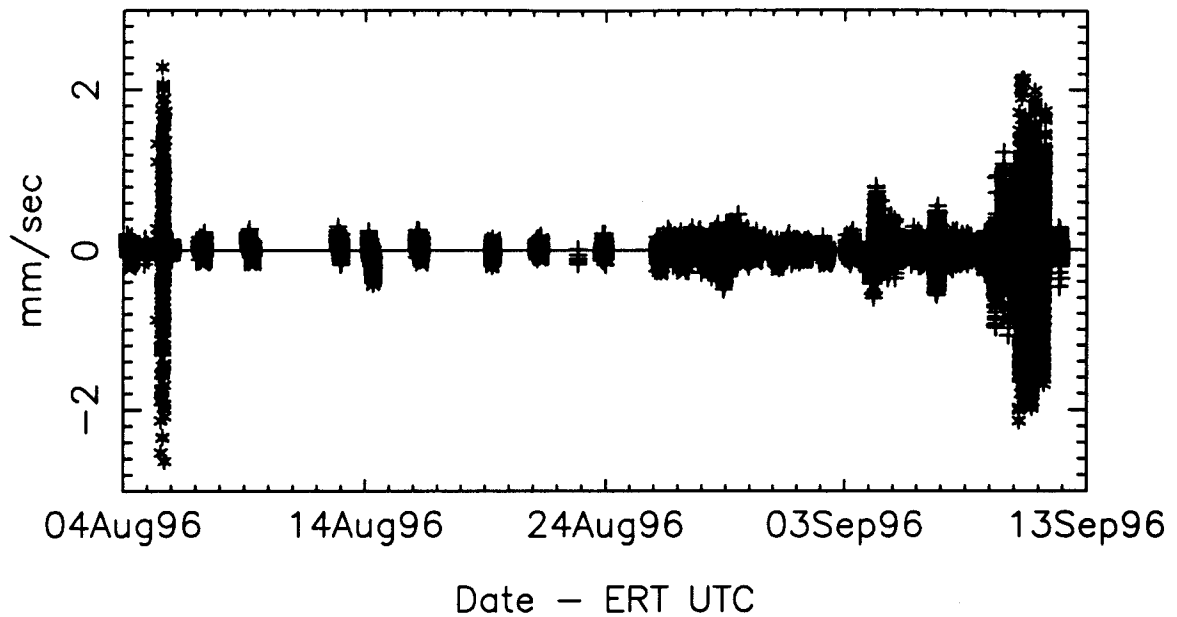


Fig. 2b Doppler Residuals – Ganymede 2 encounter

No.= 340 rms= 0.219779

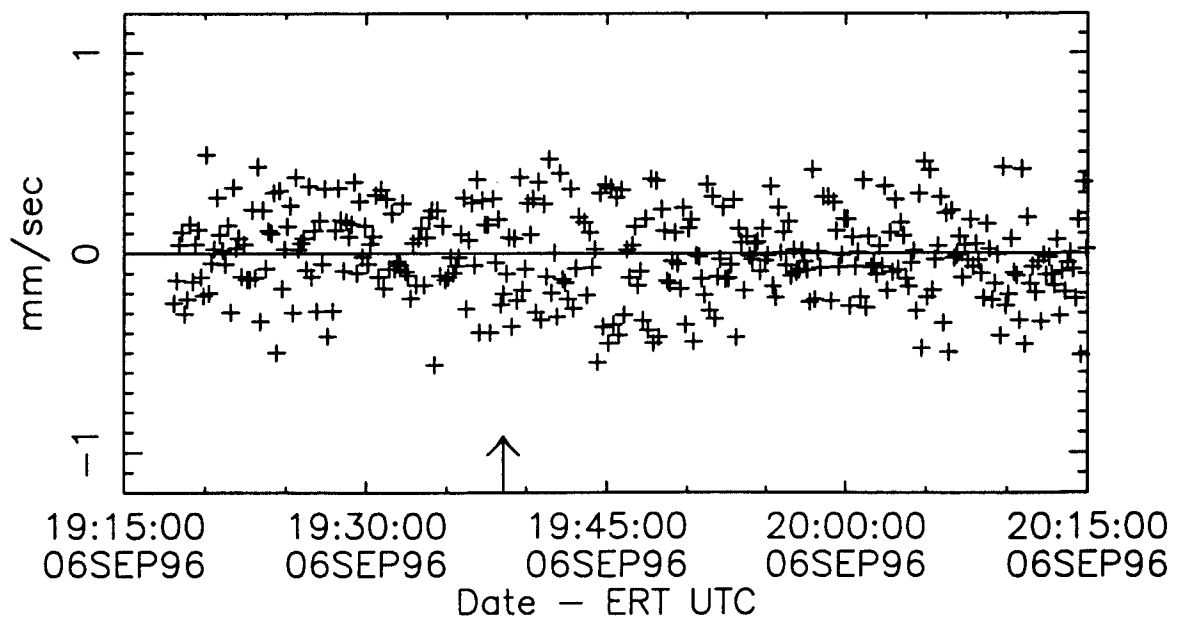


Fig. 3a Doppler Residuals – Callisto orbit 10

No.= 34277 rms= 0.291044

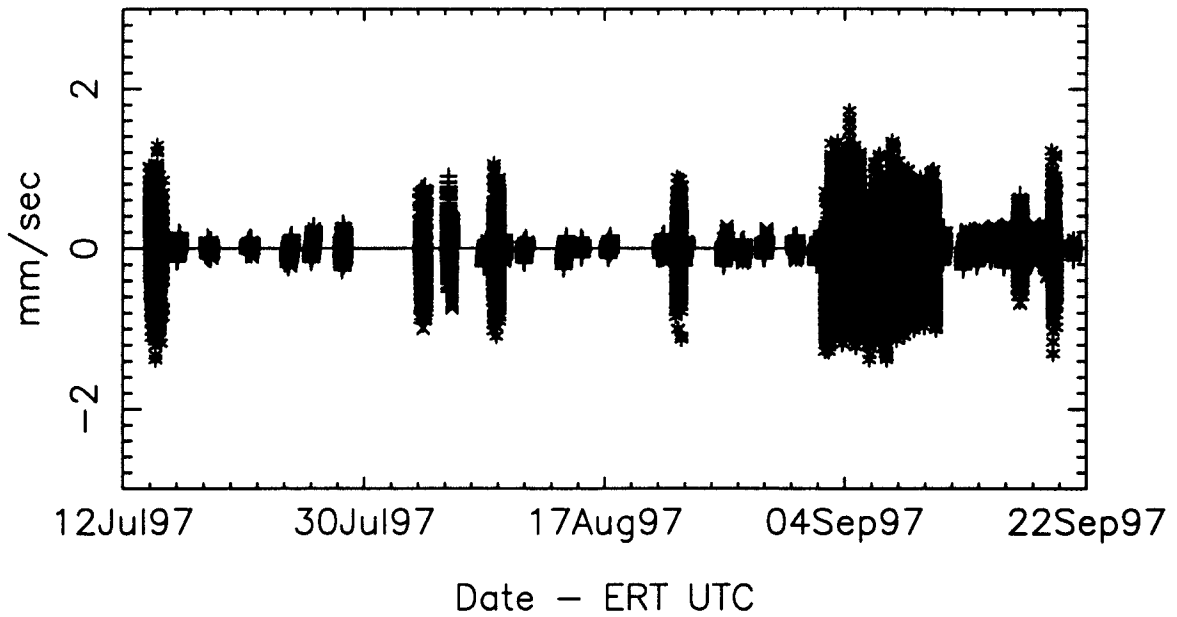


Fig. 3b Doppler Residuals – Callisto 10 encounter

No.= 652 rms= 0.230667

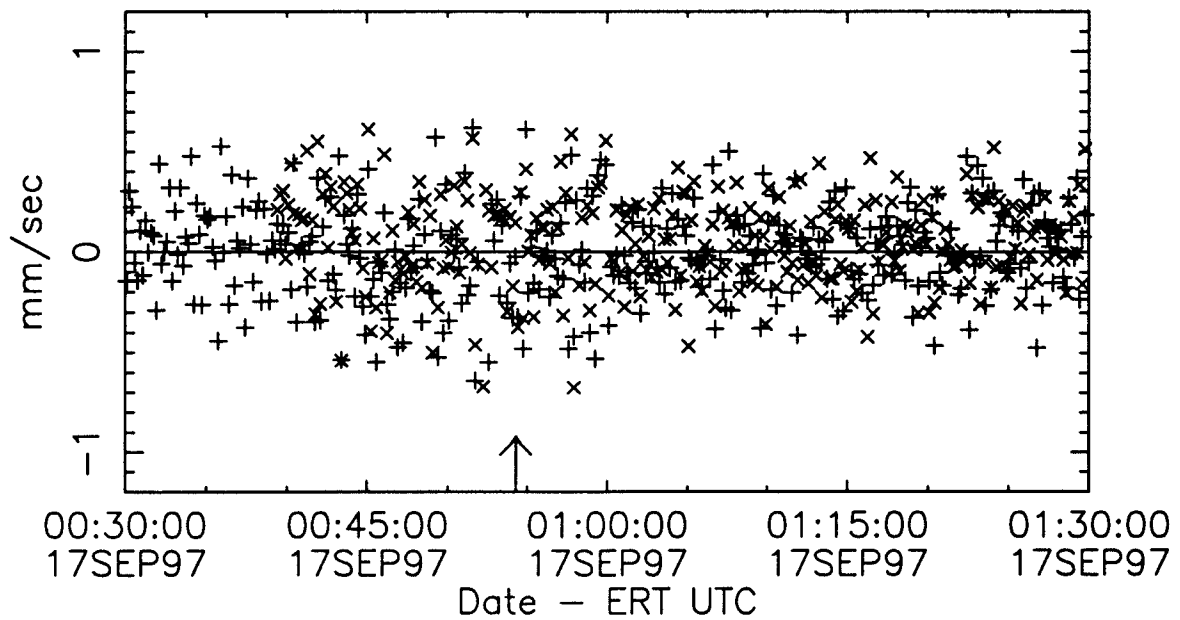


Fig. 4a Doppler Residuals — Europa orbit 12

No.= 14699 rms= 0.342057

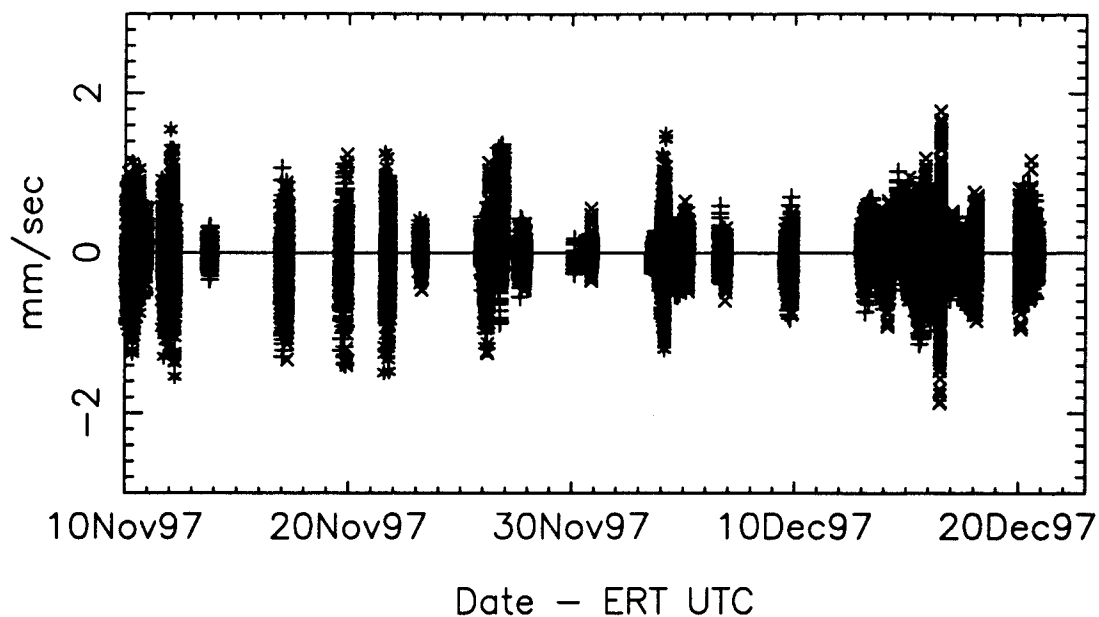


Fig. 4b Doppler Residuals — Europa 12 encounter

No.= 308 rms= 0.646717

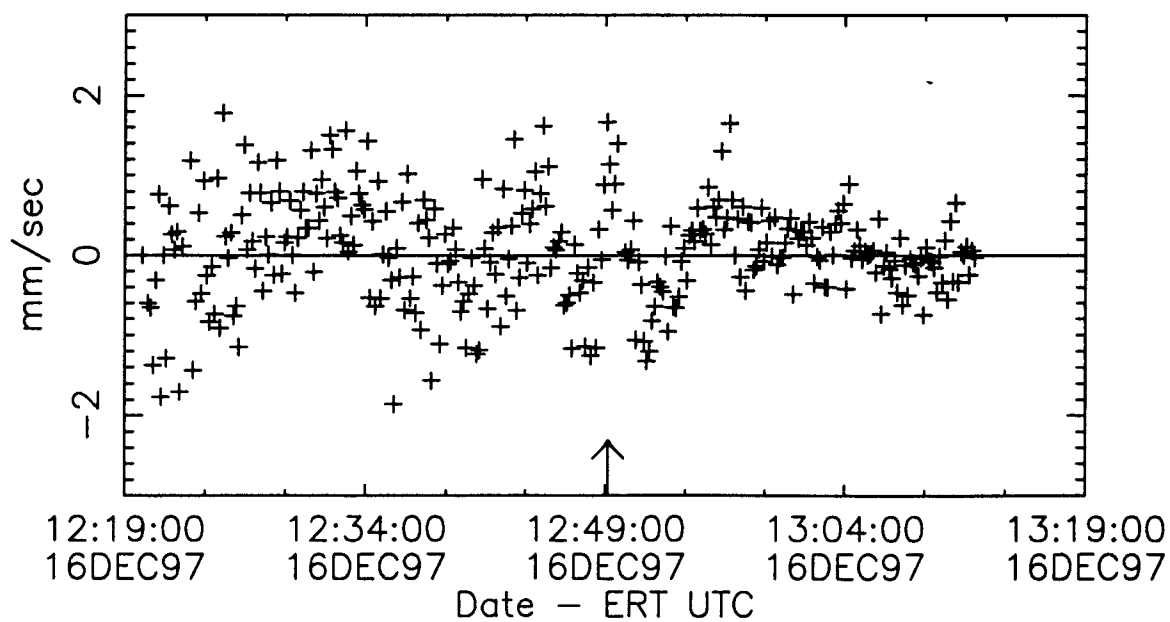


Fig. 5a Galileo Spacecraft Downtrack Differences

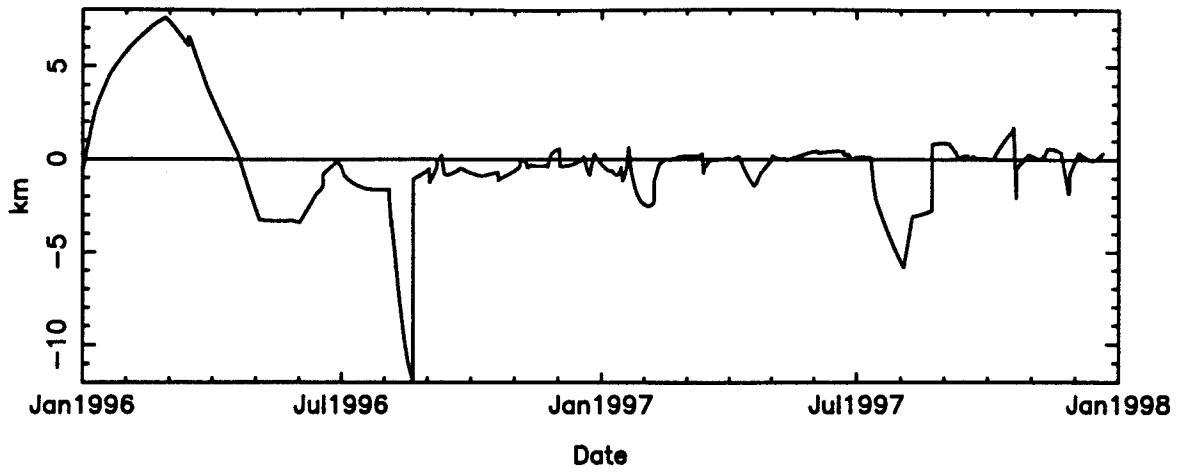


Fig. 5b Galileo Spacecraft Radial Differences

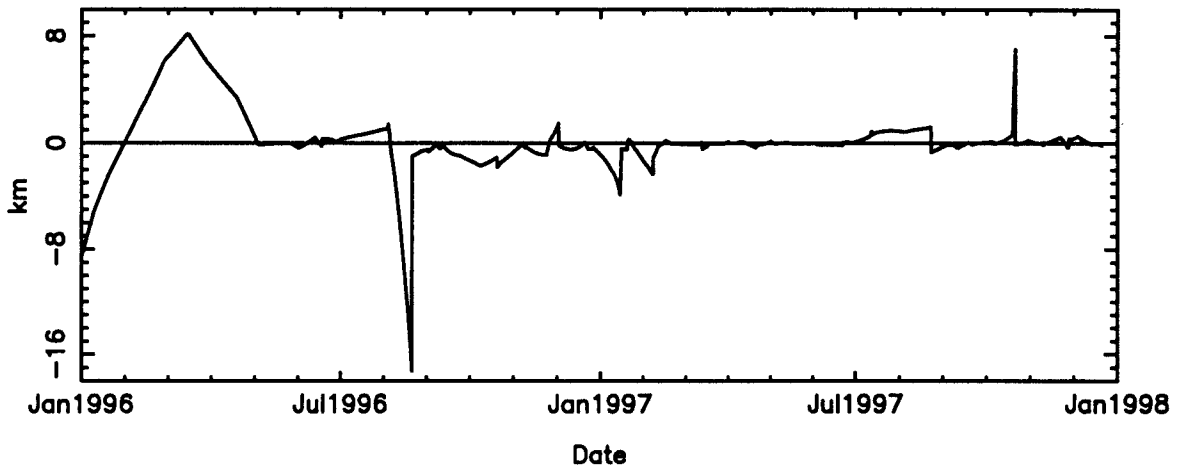


Fig. 5c Galileo Spacecraft Out-of-plane Differences

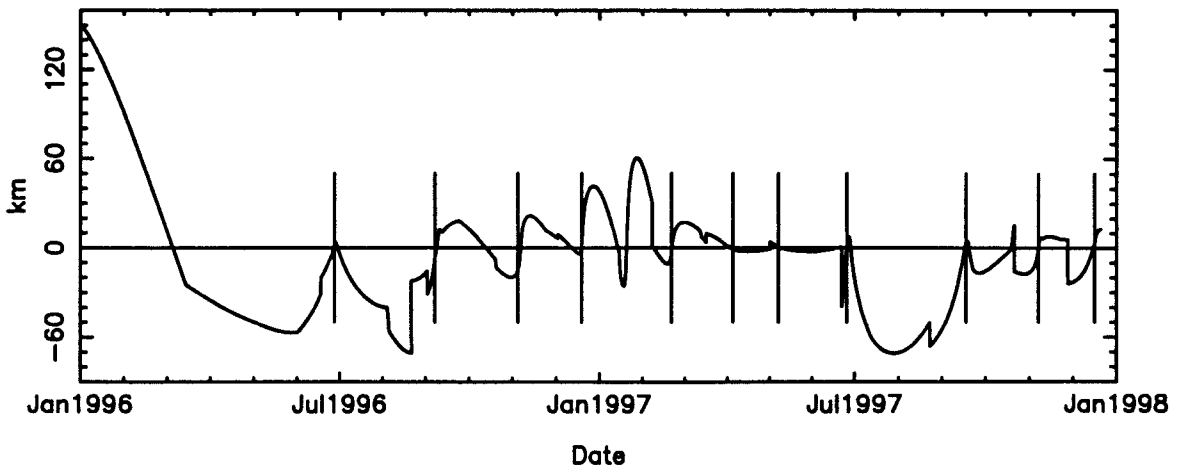


Fig. 6a Jupiter Downtrack Differences

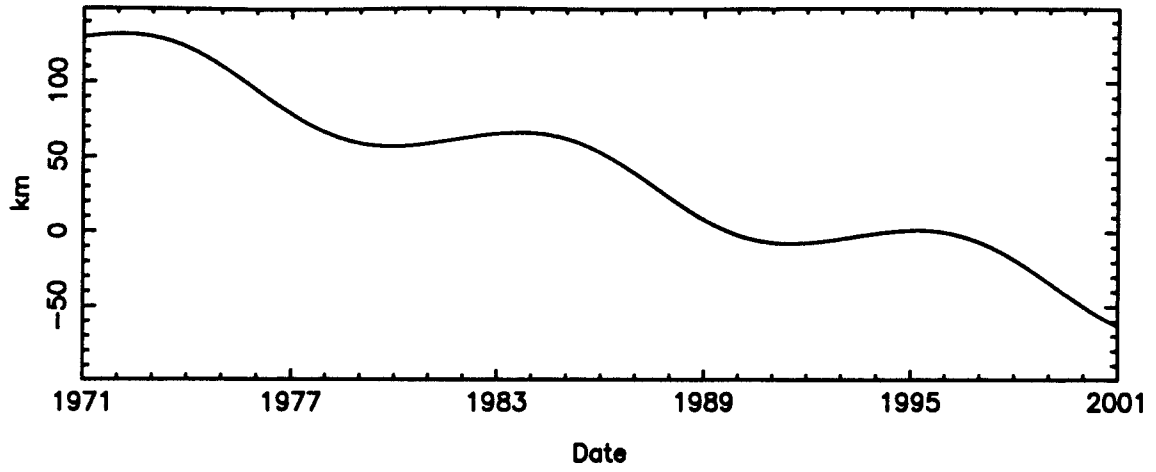


Fig. 6b Jupiter Radial Differences

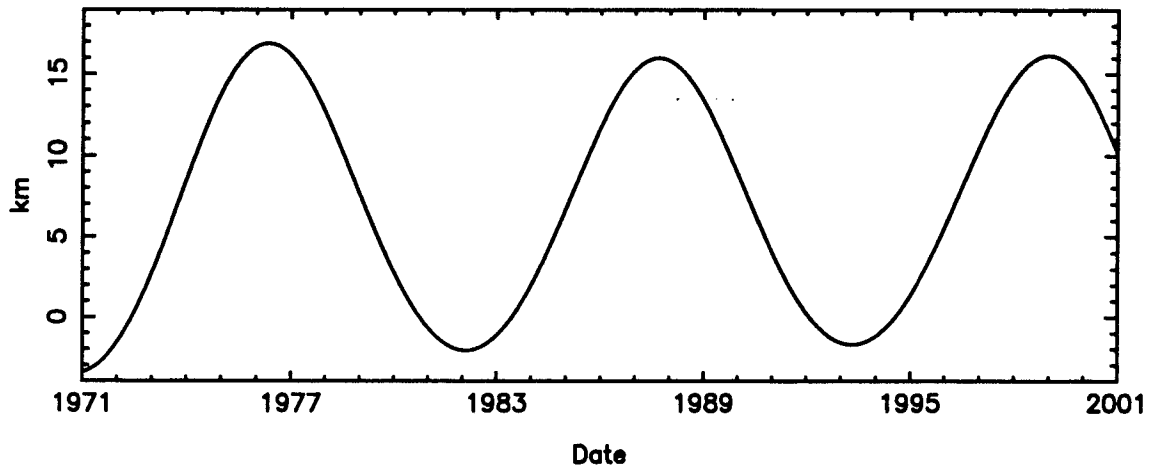


Fig. 6c Jupiter Out-of-plane Differences

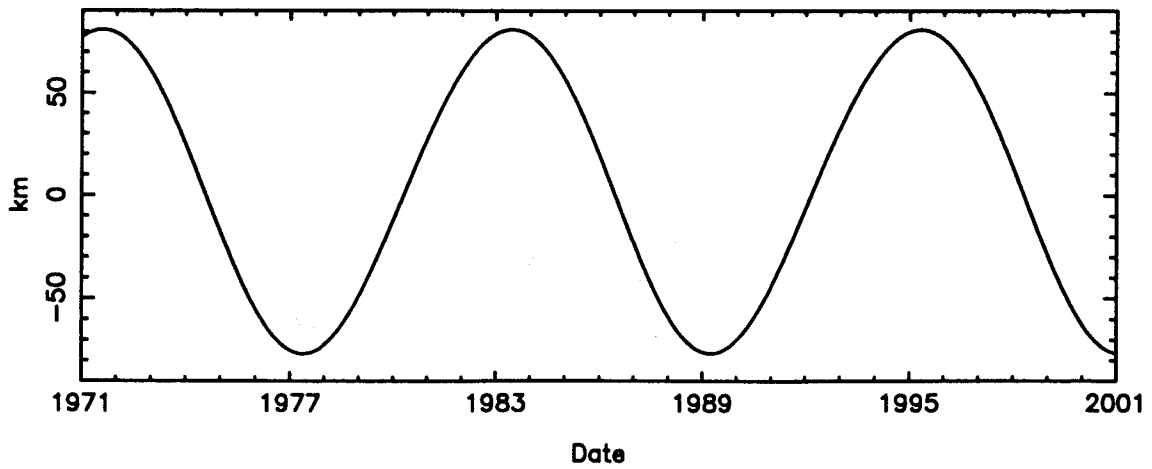


Fig. 8a Europa Downtrack Differences

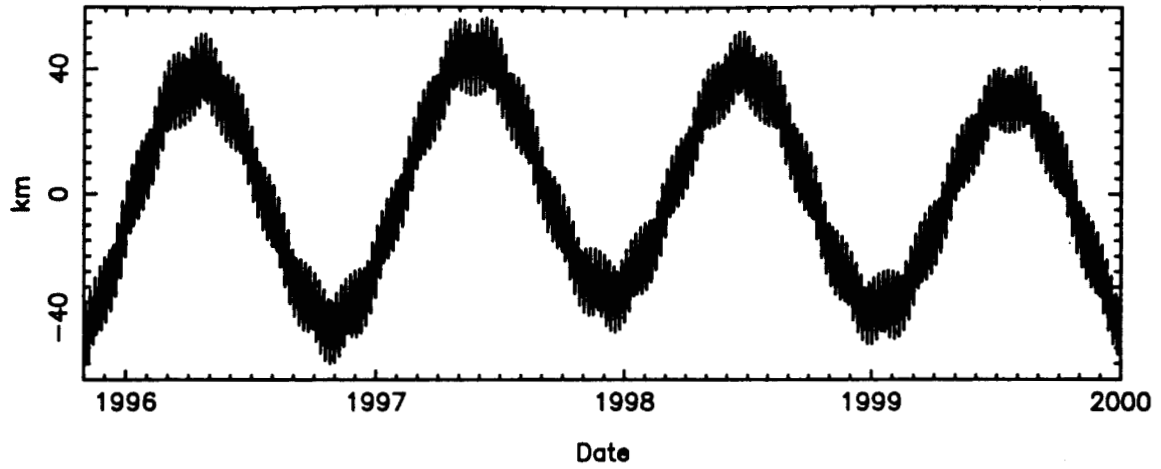


Fig. 8b Europa Radial Differences

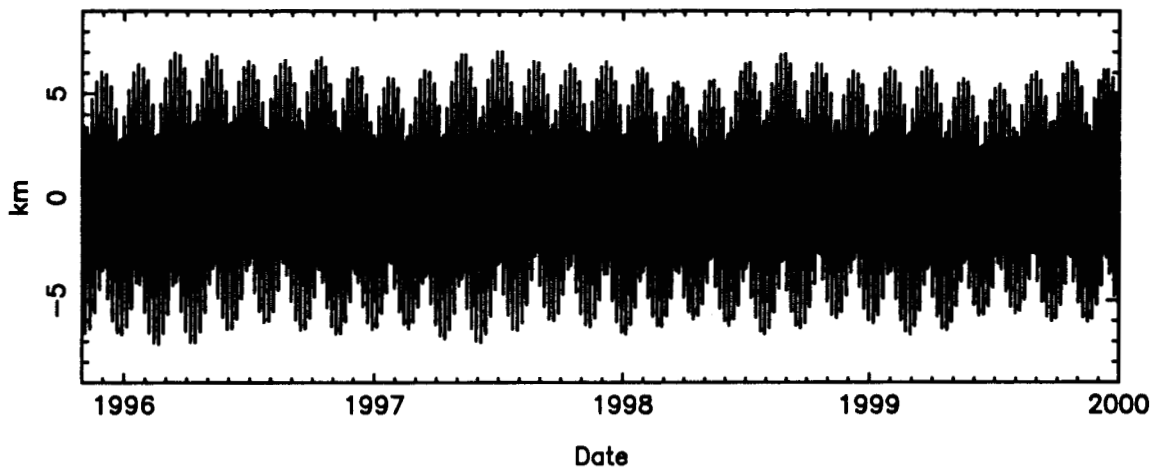


Fig. 8c Europa Out-of-plane Differences

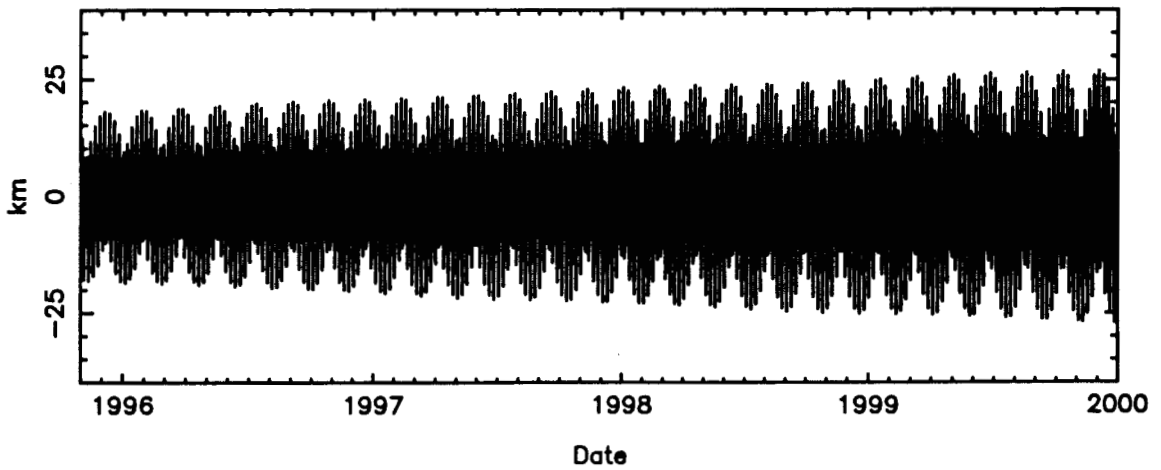


Fig. 10a Callisto Downtrack Differences

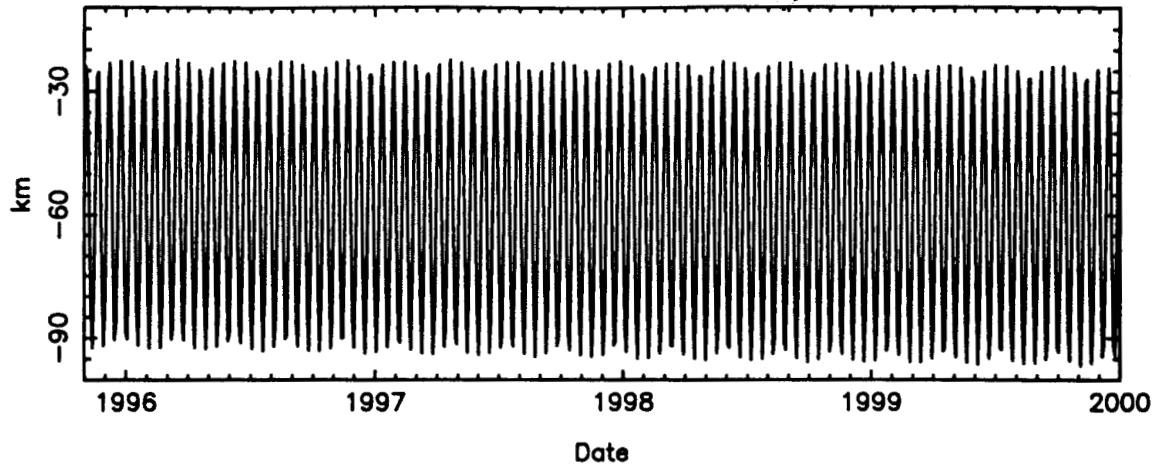


Fig. 10b Callisto Radial Differences

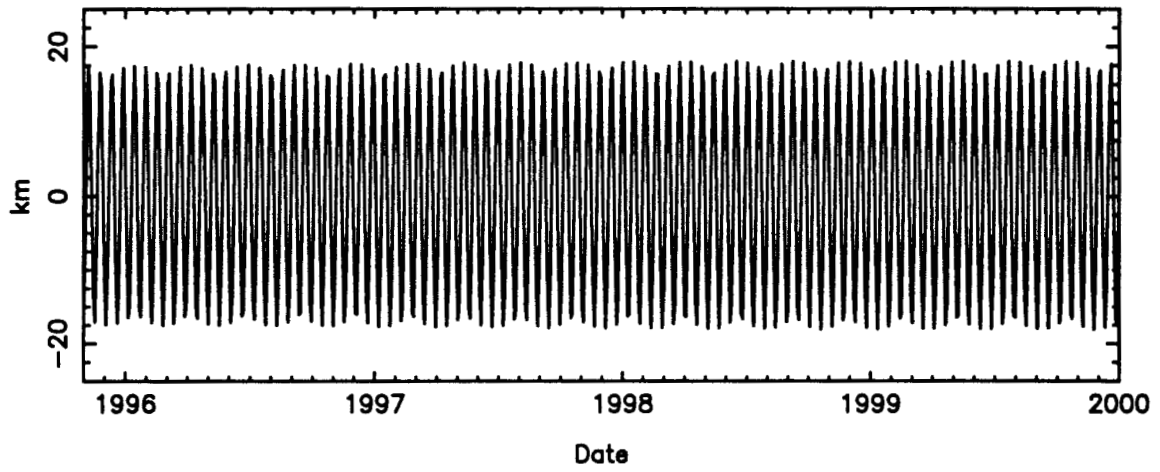


Fig. 10c Callisto Out-of-plane Differences

